Lift Force on an Aerofoil
(lab experiment)

Jiaqi, Yao*

October 19, 2023

1 Outline

In this laboratory experiment, the focus is on determining the lift force acting on an aerofoil using the Air Flow bench in a vertical wind tunnel. By examining the pressure distribution across the aerofoil's surface at varying angles of attack, the experiment aims to relate this pressure to the overall lift produced by the aerofoil.

2 Theory

Lift on an aerofoil is crucial for aircraft elevation, which can be interpreted by the Coanda effect and the different pressures between top and bottom surfaces.

For a symmetric aerofoil at zero angle, the lift generated is zero. After increasing the angle of the aerofoil, the pressure variability and producing more lift.

However, at significant angles, the airflow over the top of the wing can detach due to boundary layer effects, altering the pressure distribution and resulting in lower lift coefficients.This phenomenon is known as ”stalling”. The experimental equipment is shown in the Figure 2.1.

3 Method

*jy431@exeter.ac.uk

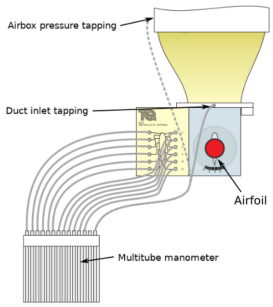

Figure 2.1: Pressure tappings for AF18 Experiment

a. An accurate value for the density of air was determined using room temperature and atmospheric pressure.

b. With the aerofoil positioned at a 0° angle of attack, pressure measurements were recorded.

c. The effective static pressure should be computed by using the atmospheric and duct inlet pressures.

d. Using the effective static pressure (p_{eff}) and the airbox pressure reading, calculate the free stream velocity and determined the Reynolds number with chord length.

e. For each pressure tapping reading, the corresponding value of pressure ratio($C_{p,n}$) was calculated, and these values were plotted against ($\frac{x}{c}$). The curves were extended to represent a chord ratio of 0 and 1. Noticed that the pressure coefficient near the leading edge is approaching zero, which indicate the directing of the air is disappeared at this point. The exact position of this stagnation point changes with incident angle.

f. From the generated curves of C_p, the lift coefficient (C_L)can be numerically integrated to derive its value.

g. The measurements have been repeated for increasing angles of attack (in steps of $5°$) up to $25°$, with additional measurements at $17.5°$ and $22.5°$. Following this, the lift coefficients were computed and a graph illustrating C_L vs. α for the aerofoil was plotted.

4 Results

The density of mercury and air and atmospheric pressure at this time can be determined from the thermometers ($23.5°$) and manometers($754mmHg$).

The air and mercury densities are ($1.2kg/m^3$and $13.534 \times 10^3 kg/m^3$) and the atmospheric pressure is ($100107.4792Pa$), as shown by equation $P_a = \rho gh$ (mercury) and by consulting the density - temperature table of mercury.

The following Table 4.1 shows the data recorded from the experiment.

Table 4.1: Raw data in experiments (Unit: mm)

Degree/Pitot No.	1	3	5	7	9	11	2	4	6	8	10	12	Atm	Airbox	Inlet
0°	196	158	152	158	167	177	184	156	155	164	170	182	186	244	190
5°	236	195	175	175	178	182	124	118	132	148	168	180	186	244	192
10°	146	220	197	187	188	187	58	88	106	146	164	180	186	244	194
15°	244	235	212	199	194	189	13	54	116	146	166	178	186	244	198
17.5°	242	239	217	203	196	190	8	42	119	148	165	178	186	244	200
20°	247	236	217	205	197	190	156	154	154	153	154	158	186	244	210
22.5°	248	238	220	209	200	192	164	162	162	160	160	162	186	244	214
25°	247	242	226	217	205	196	172	170	169	168	164	164	186	246	218

5 Analysis

Next the experimental data were processed. Firstly the difference in water head was calculated for each sampling point on tapping position by using the Pitot tube at atmospheric pressure as a standard value. The difference in water head was then converted to a difference in pressure by equation $P_n = \rho g h$, as shown in Table 5.1 below.

Table 5.1: Preliminary processing of experimental data (Unit: Pa)

Degree/Pitot No.	1	3	5	7	9	11	2	4	6	8	10	12	Atm	Airbox	Inlet
0°	98.1	-274.68	-333.54	-274.68	-186.39	-88.29	-19.62	-294.3	-304.11	-215.82	-156.96	-39.24	0	568.98	39.24
5°	490.5	88.29	-107.91	-107.91	-78.48	-39.24	-608.22	-667.08	-529.74	-372.78	-176.58	-58.86	0	568.98	58.86
10°	-392.4	333.54	107.91	9.81	19.62	9.81	-1255.68	-961.38	-784.8	-392.4	-215.82	-58.86	0	568.98	78.48
15°	568.98	480.69	255.06	127.53	78.48	29.43	-1697.13	-1294.92	-686.7	-392.4	-196.2	-78.48	0	568.98	117.72
17.5°	549.36	519.93	304.11	166.77	98.1	39.24	-1746.18	-1412.64	-657.27	-372.78	-206.01	-78.48	0	568.98	137.34
20°	598.41	490.5	304.11	186.39	107.91	39.24	-294.3	-313.92	-313.92	-323.73	-313.92	-274.68	0	568.98	235.44
22.5°	608.22	510.12	333.54	225.63	137.34	58.86	-215.82	-235.44	-235.44	-255.06	-255.06	-235.44	0	568.98	274.68
25°	598.41	549.36	392.4	304.11	186.39	98.1	-137.34	-156.96	-166.77	-176.58	-215.82	-215.82	0	588.6	313.92

Based on the Table 5.1, it was able to calculate the effective static pressure (p_{eff}) in different angle by given Equation 5.1.

$$p_{eff} = p_0 + \frac{85}{135} \times (p_a - p_0) \tag{5.1}$$

(P_0 is the inlet pressure) And calculate free stream velocity U_∞ by given Equation 5.2 in different angle.

$$U_\infty = \sqrt{\frac{2 \times (p_{airbox} - p_{eff})}{\rho}} \tag{5.2}$$

The results are shown in the following Table 5.2. And from Equation 5.3,

$$C_{p,n} = \frac{p_n - p_{eff}}{\frac{1}{2}\rho u_\infty^2} \tag{5.3}$$

the pressure ratio in different angle can be calculated. Additionally, the tapping position and aerofoil chord for the different sampling points can be obtained from the appendix which is in handbook, and the x/c

can be calculated. The initial and final points of the curves (0, 0) and (1, 0) have been added to the figures according to the lab handbook. The images are connected by using a smooth curve (Piecewise Cubic Hermite Interpolating Polynomial) as shown in Table 5.3.[1]

Table 5.2: p_{eff} and U_∞ in different angle (Unit: Pa and m/s)

Pitot No.	0	5	10	15	17.5	20	22.5	25
p_eff	24.70667	37.06	49.41333	74.12	86.47333	148.24	172.9467	197.6533
U_∞	30.11847	29.77471	29.42693	28.71875	28.35803	26.48081	25.69155	25.52602

Table 5.3: Pressure ratio (C_p) in different angle and degree

Pitot No.	1	3	5	7	9	11	2	4	6	8	10	12
x/c	0.016	0.071	0.175	0.317	0.510	0.698	0.032	0.119	0.230	0.413	0.603	0.794
0	0.135	-0.560	-0.613	-0.505	-0.342	-0.162	-0.036	-0.541	-0.559	-0.397	-0.288	-0.072
5	0.852	0.110	-0.203	-0.203	-0.148	-0.074	-1.143	-1.254	-0.996	-0.701	-0.332	-0.111
10	-0.850	0.585	0.208	0.019	0.038	0.019	-2.417	-1.850	-1.510	-0.755	-0.415	-0.113
15	1.000	0.913	0.515	0.258	0.159	0.059	-3.430	-2.617	-1.388	-0.793	-0.396	-0.159
17.5	0.959	1.019	0.630	0.346	0.203	0.081	-3.619	-2.928	-1.362	-0.773	-0.427	-0.163
20	1.070	1.103	0.723	0.443	0.256	0.093	-0.699	-0.746	-0.746	-0.769	-0.746	-0.653
22.5	1.099	1.223	0.842	0.570	0.347	0.149	-0.545	-0.594	-0.594	-0.644	-0.644	-0.594
25	1.025	1.340	1.004	0.778	0.477	0.251	-0.351	-0.401	-0.427	-0.452	-0.552	-0.552

Based on Table 5.3, Pressure distributions are plotted as a graph of the pressure ratio, which at 8 different angles with x/c as the x-axis and C_p as the y-axis. The figure is shown in Figure 5.1. By using the Equation 5.4, We can calculate lift coefficient C_L.

$$C_L = \frac{F_L}{\frac{1}{2}\rho U^2 A} \tag{5.4}$$

Noticed that A is the plan area of the aerofoil. By using mathematical method, this can be evaluated by given equation:

$$C_L = \int \left[C_{pl}\left(\frac{x}{c}\right) - C_{pu}\left(\frac{x}{c}\right) \right] d\left(\frac{x}{c}\right)$$

However, an important point to note is that a direct integration requires a continuous function. In order to find the solution, we use discrete data points to evaluate the C_L by using trapezoidal rule. So, the discrete version of the integral becomes:

$$\Delta C_L = \sum \left(\frac{C_{pl,i+1} + C_{pl,i}}{2} - \frac{C_{pu,i+1} + C_{pu,i}}{2} \right) (x_{i+1} - x_i)$$

Where i is the index of the data points. The results show in Table 5.4 and Figure 5.2.

[1] Regression analysis is not applicable to smooth curve fitting.

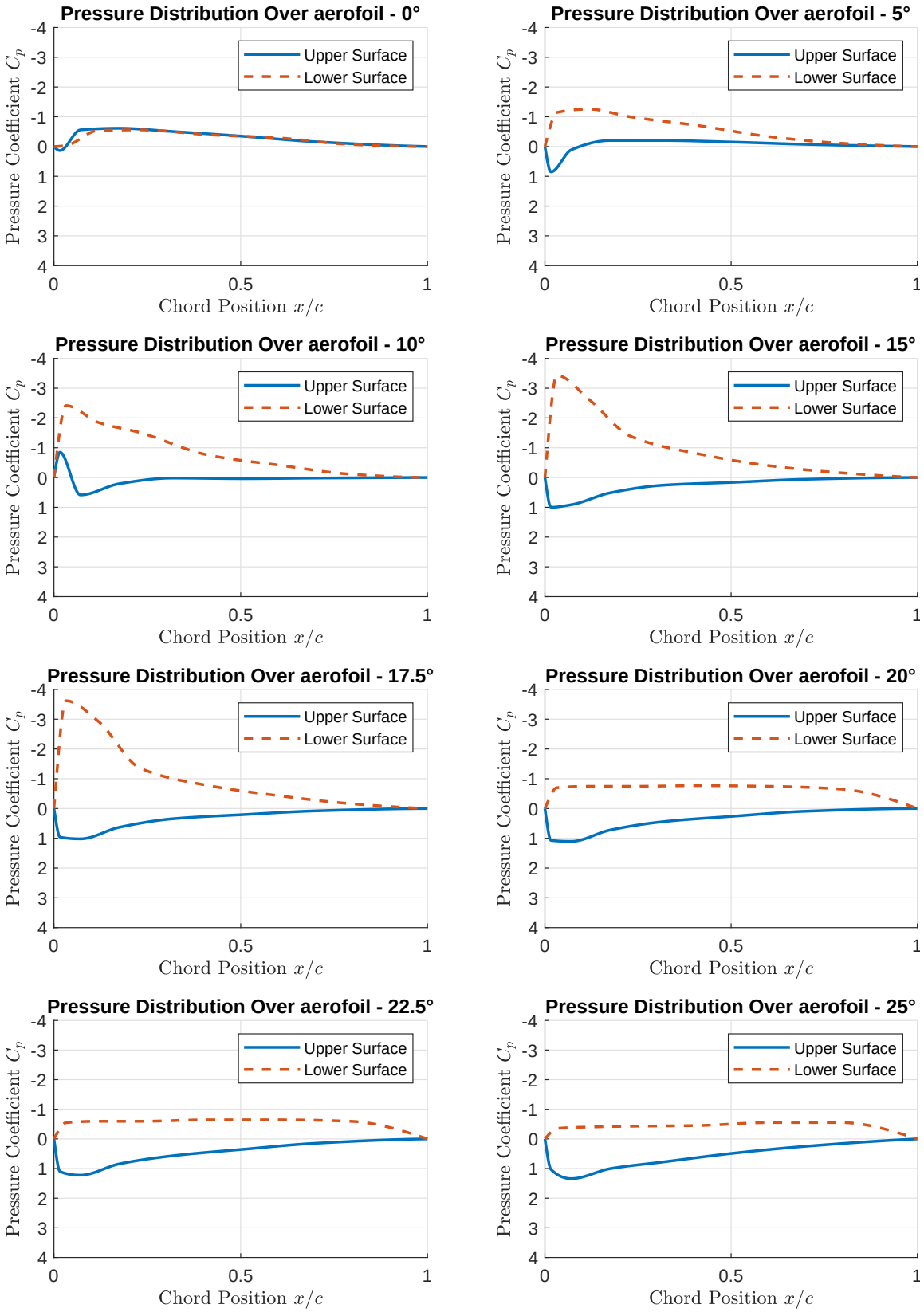

Figure 5.1: Pressure distribution over aerofoil

Table 5.4: Lift coefficient (C_L) in different angle

Degree	0	5	10	15	17.5	20	22.5	25
C_L	-0.040	0.383	0.676	0.939	1.015	0.840	0.828	0.830

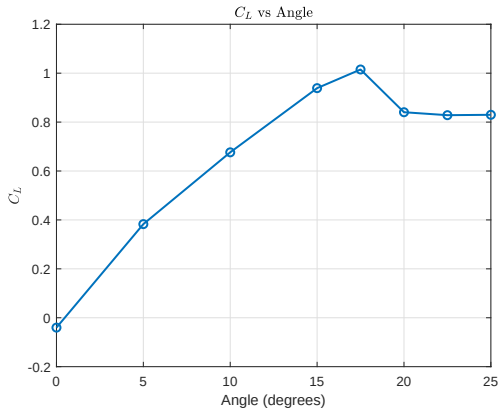

Figure 5.2: C_L vs Angle

Error Analysis

Error analysis is very important which means the systematic evaluation of the uncertainties or inaccuracies in measurements and calculations, helping to understand the sources and implications of potential deviations from true values. The possible errors in the experiment are:

1. Mercury density and air density are not accurate.
2. The trapezoidal rule is using discrete point to evaluate the integral, which occur the error.
3. Pitot tube not sealing well and leaking air.

Some examples of potential errors are given above. The first and third of these are systematic errors and the second is a random error. Systematic errors can only be improved by improving the accuracy of the measuring equipment. Next, the focus is on analysing the random errors due to the trapezoidal integration method. The trapezoidal integration method uses a linear connection for integration, which can be optimised by first connecting the discrete points with a smooth curve (Piecewise Cubic Hermite Interpolating Polynomial) and then using the different integration method to approximate the true value. The results is in Table 5.5. [2]

6 Conclusions

[2]The error percentages are calculated based on the values of the Trapezoidal method.

Table 5.5: Different integration method to calculate C_L

Degree	0	5	10	15	17.5	20	22.5	25
Trapezoidal	-0.040	0.383	0.676	0.939	1.015	0.840	0.828	0.830
Simpson's Rule	-0.0206	0.4612	0.8561	1.1218	1.2110	0.9162	0.8964	0.8975
Error (Simpson's)	48.5%	20.4%	26.6%	19.5%	19.4%	9.1%	8.3%	8.1%
Romberg's method	-0.0228	0.4606	0.8634	1.1261	1.2179	0.9181	0.8989	0.9006
Error (Romberg's)	43.0%	20.3%	27.7%	19.9%	20.0%	9.3%	8.5%	8.5%

Based on the Figure 5.1 the pressure distribution over the aerofoil for both the upper and lower surfaces demonstrates significant variations across different chord positions. The pressure coefficients on the upper surface tend to have more negative values as compared to the lower surface, indicating a higher velocity of flow and consequently a lower pressure. Furthermore, the Figure 5.2 showcases the lift coefficient's relationship with the angle of attack. An initial increase in the lift coefficient is observed as the angle of attack rises. However, after reaching a peak, the lift coefficient appears to plateau or slightly decrease.

In conclusion, the pressure distribution patterns on the aerofoil validate the principles of aerodynamics and the generation of lift. The relationship between lift coefficient and angle of attack is crucial in understanding the performance and efficiency of the aerofoil, indicating the importance of optimizing the angle for maximum lift and avoiding angles that could lead to diminished performance or stalling.

About error analysis, as the degree increases, the error percentages for both Simpson's Rule and Romberg's method generally decrease, indicating that the accuracy of these integration methods improves at higher degrees. In order to get more accurate results, we need to conduct more experiments to reduce the error and calculate more accurate values.

Question in handbook

• Can you explain why the aerofoil has to be thin?

Calculation of p_{eff} is based on the pressure at the outlet and the head difference (85/135mm) in Equation 5.1. Since p_{eff} is sufficient for thin, the default air flow cross-sectional area is equal to the outlet area. When the peff has a certain thickness, the area difference factor needs to be considered, which has an impact on the experimental results.

• Near stall, the manometer readings may fluctuate significantly; why is this?

One possible reason is flow Separation and reattachment. As the angle of attack approaches the stalling angle, the flow begins to separate from the upper surface of the aerofoil which causing the pressure distribution on the surface to fluctuate. Another reason is turbulent flow. When the angle of attack approaches the stalling angle, it becomes highly turbulent which can lead to fluctuating pressure readings.